Int. J. Environ. Sci. Technol. (2014) 11:1207–1214
DOI 10.1007/s13762-013-0317-x

ORIGINAL PAPER

Kinetics of oxytetracycline sorption on magnetite nanoparticles

**S. Rakshit · D. Sarkar · P. Punamiya ·
R. Datta**

Received: 15 January 2013 / Accepted: 2 May 2013 / Published online: 17 May 2013

Abstract Iron oxide nanoparticles (nano-Fe) have been widely used in environmental remediation, including that of emerging contaminants, such as antibiotics. Magnetite nanoparticles (nano-Fe_3O_4) have been reported to form on the outer surface of nano-Fe and have the potential to be a good sorbent for certain antibiotics. This study reports, for the first time, the kinetics and thermodynamics of adsorption of a common tetracycline group antibiotic, oxytetracycline (OTC), on nano-Fe_3O_4. Batch sorption kinetics were evaluated by varying initial OTC concentration (0.25–2 mM), nano-Fe_3O_4 concentration (2.5–20 g L^{-1}), pH (3.8–7.6), temperature (5, 15, 35 °C), and ionic strength (0.01–0.5 M KCl) to derive thermodynamic and kinetic constants. Results show that OTC sorption kinetics is rapid and increases with increasing temperature. The derived thermodynamic constants suggest a surface chemical-controlled reaction that proceeds via an associative mechanism. Results indicate the potential of developing a nano-magnetite-based remediation system for tetracycline group of antibiotics.

Keywords Adsorption · Oxytetracycline · Nano-magnetite · Kinetics · Thermodynamics · Remediation

S. Rakshit (✉) · D. Sarkar · P. Punamiya
Earth and Environmental Studies Department, Montclair State University, Montclair, NJ, USA
e-mail: rakshits@mail.montclair.edu

R. Datta
Department of Biological Sciences, Michigan Technological University, 1400 Townsend Drive, Houghton, MI 49931, USA

Introduction

Increasing concentrations of antibiotics in soils, sediments, surface water, and groundwater are a major environmental concern (Hamscher et al. 2002; Kolpin et al. 2002; Schwarzenbach et al. 2006). Veterinary antibiotics (VAs) may enter the environment via different pathways such as by application of untreated manure and sewage sludge to soil, runoff from the manure stockpiles of confined animal feeding operations (CAFOs), discharge of wastewater to streams as primary sources, as well as runoff from agricultural lands as secondary sources (Boxall et al. 2003; Watkinson et al. 2007; Kummerer 2009). Human antibiotics can enter the environment via discharge from municipal sewage treatment plants, which are not equipped to treat antibiotics in wastewater. One of the major concerns with the presence of antibiotics in the environment is the possibility of growing resistance in harmful pathogens, which has prompted many fate and transport studies in the laboratory and in the field using common veterinary and human antibiotics (Chu et al. 2010; Pils and Laird 2007; Davis et al. 2006; Boxall et al. 2002; Tolls 2001; Rabolle and Spliid 2000).

Antibiotics of the tetracycline group are commonly used as effective antibacterial agents in both human and animal disease prevention (Kulshrestha et al. 2004). One of the most common antibiotics in the tetracycline group is oxytetracycline (OTC), which is used widely in CAFOs and in the treatment of various bacterial infections in humans (Rubert and Pedersen 2006). The majority of the environmental fate and transport studies aimed at understanding the equilibrium sorption behavior of OTC on soils and environmentally relevant sorbents such as soil minerals (Jones et al. 2005; Figueroa and MacKay 2005; Gu and Karthikeyan 2005; Pils and Laird 2007). Only a few researchers have emphasized the role of kinetics in developing a detailed understanding of fate and transport of OTC in the environment. Further, the role of high-capacity sorbents of environmental sorbents, such as nano-Fe, in the remediation of antibiotic-rich water has not yet been properly explored.

Iron oxide nanoparticles (nano-Fe) have been used widely for the treatment of contaminated land and water (Crane et al. 2011). Magnetite (Fe_3O_4) nanoparticles (nano-Fe_3O_4) are frequently reported to be the most common mineral formed at the outer surface of zero valent iron nanoparticles (nano-Fe^0) (Nagayama and Cohen 1962; Furukawa et al. 2002; Phillips et al. 2003; Scott et al. 2010). This prompted many researchers to evaluate the role of nano-Fe_3O_4 in contaminant removal. Although Crane et al. (2011) reported minor removal of uranium (VI) from a contaminated water by nano-Fe_3O_4, Yang et al. (2010) observed high arsenic (As) retention at acidic pH and medium to low retention at neutral to alkaline pH in the presence of nano-Fe_3O_4. In another study, Wang et al. (2011) found that As(V) can be structurally incorporated into nano-Fe_3O_4 in precipitation reaction and indicated the possibility of using nano-Fe_3O_4 as a remediation material for water decontamination process. Other than the remediation of metalloids and radioactive materials, researchers have recently reported the usefulness of nano-Fe_3O_4 in the removal of antibiotics (Zhang et al. 2011; Rakshit et al. 2013).

A previous study from our group indicated sorption of OTC to nano-Fe_3O_4 (Rakshit et al. 2013). However, a detailed kinetic evaluation has not been reported. Kinetic study can generate rate constants and pseudo-order rate coefficients, which are useful in predicting the immobilization rate of antibiotics in the presence of nano-Fe_3O_4. For example, on the basis of the rate of antibiotics sorption on soil components, it is possible to estimate the amount that will run off to surface water or percolate to groundwater during a high precipitation event. It is impossible to make such predictions based on equilibrium sorption K_d values alone. Moreover, detailed kinetic data will help design engineered treatment systems utilizing nano-Fe_3O_4 as the remediation material.

Because wide ranges of temperature fluctuations are possible in the environment, evaluation of the temperature dependence of OTC sorption kinetics is important. The 'Arrhenius Equation,' which is commonly used for this purpose, relates kinetic rate coefficients to thermodynamic parameters such as activation energy (E_a) (Scheckel and Sparks 2001). In addition to the 'Arrhenius Equation,' the 'Eyring Equation,' which relates the reaction rate constant to entropy and enthalpy of activation, is a useful guide to understand the mechanistic details of a reaction (Scheckel and Sparks 2001; Stumm and Morgan 1996). The main objectives of this study are to measure the effect of temperature on OTC sorption kinetics by nano-Fe_3O_4, and derive the thermodynamic parameters, and to formulate an empirical rate equation to predict the removal of OTC by nano-Fe_3O_4 in the environment.

Materials and methods

Materials

Nano-sized magnetite (<50 nm) was purchased and used as received from Sigma-Aldrich (St. Louis, MO, USA) (Crane et al. 2011). Detailed characterization of nano-Fe_3O_4 is available elsewhere (Crane et al. 2011). The BET surface area measured in our earlier work was about 40 $m^2\ g^{-1}$ (Rakshit et al. 2013). OTC hydrochloride, potassium chloride, and PIPES (1,4-piperazinebis(ethane sulfonic acid) were purchased from Sigma-Aldrich (St. Louis, MO, USA). HPLC grade methanol and acetonitrile were purchased from Fisher Scientific (Fairlawn, NJ, USA). For all the experiments, polypropylene centrifuge bottles were used (Fisher Scientific, Fairlawn, NJ, USA).

Transmission electron microscopy

To understand the particle morphology of nano-Fe_3O_4, TEM images were obtained with a Hitachi H-7500 TEM operating at 120 keV. Samples were dissolved in ethanol and sonicated. A drop of sample was mounted on 300-mesh copper grids. Images were collected at 80 keV. TEM image of nano-Fe_3O_4 is shown in Fig. 1, which confirmed the nano-size of magnetite particles.

Analytical

Aqueous OTC concentrations were quantified using a Finnigan Surveyor plus HPLC system (Thermo Scientific) equipped with quadruple pumps coupled with Surveyor PDA plus detector (Photodiode Array) and a Surveyor Plus autosampler. Details of procedures can be found in Rakshit et al. (2013) and in Fritz and Zuo (2007). Our earlier work indicated that a negligible amount of dissolved Fe was detected in all experiments but did not interfere with the HPLC measurements (Rakshit et al. 2013).

Batch sorption/kinetic experiments

Kinetics of batch sorption experiments were performed using 20 g L^{-1} magnetite at pH 5.55 buffered with 0.01 M PIPES with KCl as an ionic strength (I) adjuster. Use of PIPES buffer to study antibiotics sorption was reported by many researchers (Figueroa and Mackay 2005; Vasudevan

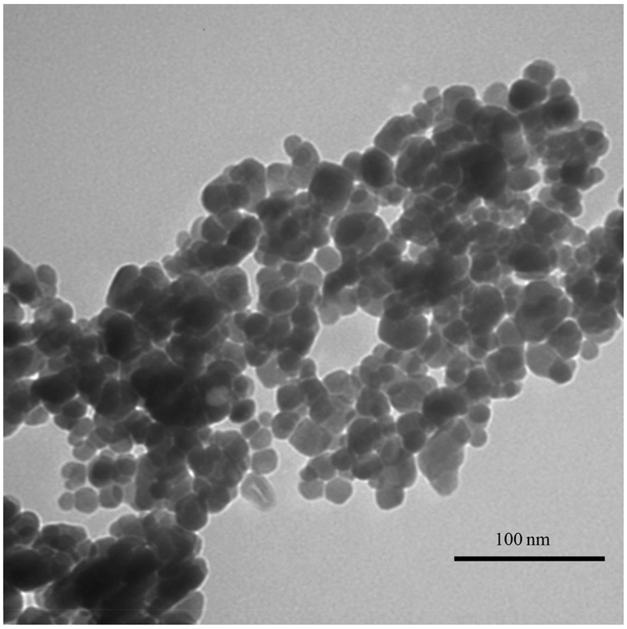

Fig. 1 TEM image of nano-Fe_3O_4

et al. 2009). To verify the mechanistic details and derive thermodynamic parameters, temperature effects on the sorption kinetics were conducted at three different temperatures (5, 15, and 35 °C) and two different I s (i.e., 0.01 and 0.5 M KCl) at a constant pH of 5.55 and initial OTC concentrations of 2 mM. The temperature was controlled using a circulating water bath (VWR Scientific, Model 1167P, Cat No. 13271-082) connected to a jacketed beaker, which was fitted to a horizontal shaker (Orbital Shaker 57018-754, VWR Scientific; shaken at 200 rpm). Suspension samples were removed from the reaction mixture periodically and filtered with 0.2-μm syringe filters (Fisher Scientific, 09-730-19) prior to analysis. A final equilibration time of 24 h was chosen (Rakshit et al. 2013). For the determination of the reaction order, several kinetic experiments were carried out by varying initial OTC concentrations (0.25–1 mM), solid concentrations (2.5–20 g L^{-1}), and pH (3.8–7.6) at a laboratory ambient temperature (25 °C). Since the initial sorption step was very fast, data were fitted starting from 10 min until 6 h. A similar observation and method of kinetic data analysis was done by Wehrli et al. (1990) in the case of vanadyl (IV) sorption on aluminum oxide. The method of initial slope and isolation was used for all the kinetic data analysis (Lasaga 1981). All experiments were conducted in duplicate and mean values were reported. Earlier work indicated that magnetite did not undergo any redox reaction with OTC (Rakshit et al. 2013). In addition, OTC sorption was similar in both oxic and anoxic conditions. Therefore, all experiments were conducted in oxic conditions. For all the experiments, a control was included where OTC was spiked in the same reaction mixture but nano-Fe_3O_4 to identify any potential degradation of OTC with time in the absence of nano-Fe_3O_4.

Kinetic analysis

A generalized rate equation of the type:

$$-d[\mathrm{OTC}]/\mathrm{d}t = k\,[\mathrm{OTC}]^x[\mathrm{XOH}]^y[\mathrm{H}^+]^z \tag{1}$$

was used, where d[OTC]/dt is the rate of the loss of OTC from the solution, k is the rate constant, [OTC] is the concentration of OTC, [XOH] is the concentration of magnetite surface sites, and [H^+] is the concentration of proton. The reaction orders for OTC, XOH, and H^+ are x, y, and z, respectively. At an excess of [XOH] and at constant pH, Eq. (1) is reduced to:

$$-d[\mathrm{OTC}]/\mathrm{d}t = k_1[\mathrm{OTC}]^x \tag{2}$$

where $k_1 = k\,[\mathrm{XOH}]^y[\mathrm{H}^+]^z$.

Logarithmic transformation of Eq. (2) results in:

$$\log\left(-d[\mathrm{OTC}]/\mathrm{d}t\right) = x\log[\mathrm{OTC}] + \log k_1 \tag{3}$$

A plot of log ($-d$[OTC]/dt) versus log [OTC] results in a slope of x. In a similar fashion, y and z can be determined. For all the kinetic analysis, the method of initial rate and isolation was used (Lasaga 1981). A rate equation similar to Eq. (1) was used for the sorption study (Wehrli et al. 1990).

Thermodynamic parameters

Arrhenius equation was used to analyze the effect of temperature on reaction kinetics:

$$k = A\,\mathrm{e}^{(-E_a/RT)} \tag{4}$$

where k is the reaction rate coefficient, A is the pre-exponential factor, E_a is the activation energy of the reaction, R is the universal gas constant (8.314 J mol^{-1} K^{-1}), and T is the temperature in absolute scale (Kelvin). A simple transformation of Eq. (4) results in a linearized form:

$$\ln k = -E_a/RT + \ln A \tag{5}$$

ln k versus $1/T$ was plotted, and from the slope ($-E_a/RT$), activation energy E_a was determined. Activation energy higher than 42 kJ mol^{-1} indicates a surface chemical-controlled reaction (Sparks 1989).

For the determination of enthalpy, entropy, and Gibbs free energy of activation, the Eyring equation was employed. A linearized form of the Eyring equation is given below:

$$\ln(k/T) = \ln(k_b/h) + \left(\Delta S^{\ddagger}/R\right) - \Delta H^{\ddagger}/RT \tag{6}$$

where k is the reaction rate coefficient, T is the absolute temperature in Kelvin, k_b is the Boltzmann constant (1.380658×10^{-23} J K^{-1}), h is the Planck's constant ($6.6260755 \times 10^{-34}$ J s), R is the universal gas constant (8.314 J mol^{-1} K^{-1}), $\Delta S^{\ddagger}$ is the standard entropy of activation, and $\Delta H^{\ddagger}$ is the standard enthalpy of activation. The $\Delta H^{\ddagger}$ was determined by plotting ln (k/T) versus $1/T$ with a slope of $\Delta H^{\ddagger}/R$. The $\Delta S^{\ddagger}$ was calculated from the intercept [ln (k_b/h) + ($\Delta S^{\ddagger}/R$)].

In addition to the Arrhenius and Eyring equations, the van't Hoff equation was used to derive thermodynamic parameters:

$$\ln K_{\mathrm{ad}} = -\Delta H_{\mathrm{ad}}/RT + \Delta S_{\mathrm{ad}}/R \quad (7)$$

Equation (7) can also be written as:

$$\ln K_{\mathrm{d}} = -\Delta H_{\mathrm{ad}}/RT + \Delta S_{\mathrm{ad}}/R \quad (8)$$

Equation (8) has been used by many researchers to analyze temperature effects on the K$_{\mathrm{d}}$ value (Chang et al. 2009). A plot of ln K_{d} versus $1/T$ will result in a slope of $\Delta H_{\mathrm{ad}}/R$ and an intercept of $\Delta S_{\mathrm{ad}}/R$. van't Hoff equation assumes that both ΔH_{ad} and ΔS_{ad} are independent of temperature. Alternatively, the value of ΔH_{ad} and ΔS_{ad} can be calculated from the following equation:

$$\ln (K_{\mathrm{d2}}/K_{\mathrm{d1}}) = \Delta H_{\mathrm{ad}}/R\,[(T_2 - T_1)/T_2T_1] \quad (9)$$

where K_{d2} is the equilibrium constant determined at temperature T_2, and K_{d1} is the equilibrium constant at temperature T_1.

Results and discussion

Temperature effects on OTC sorption kinetics

Temperature had a profound effect on OTC sorption kinetics by magnetite at both I s studied (i.e., $I = 0.01$ and 0.5 M KCl) (Fig. 2a, b). A first-order kinetic fit was reasonable for both I s and had R^2 values ranging from 094 to 0.99 (Table 1). It was necessary to convert the concentration unit to M and time unit to s for further analysis by the Arrhenius and Eyring equations. The calculation of pseudo-first-order rate coefficients from any other concentration and time units would generate wrong Arrhenius and Eyring parameters (Keleti 1983). None of the control experiments indicated any loss of OTC from solution at all three temperatures indicating negligible dissipation of OTC at these temperatures (data not shown). At low temperatures (5 and 15 °C), sorption kinetics was slower than at high temperature (35 °C) at both I s (Table 1). The increase in temperature from 5 to 35 °C enhanced the reaction rate by approximately four times and ten times for I s 0.01 and 0.5 M, respectively (Table 1). This could be explained by the activation energy calculated from the Arrhenius equation for $I = 0.01$ and 0.5 M. It is clear from the E_{a} values that at $I = 0.5$ M, the energy barrier is somewhat higher than at $I = 0.01$ M (Table 2; Fig. 2a, b). Therefore, when sufficient energy is available at higher temperature, the sorption kinetics increased dramatically in the case of high I. The mechanistic explanation of this phenomenon may be complex. Generally, background electrolyte concentrations affect sorption in two ways: (1) by changing the surface charge and (2) by affecting the competition between the electrolyte ions and the sorbing anions (Hays et al. 1988). Because our experiments were conducted at a pH value of 5.55 where the magnetite surface most likely had a positive surface charge, a higher electrolyte concentration would neutralize the positive surface charge and a greater force to bring OTC close to the magnetite surface would be required for sorption. In addition, at higher I, more competition between electrolyte ions and OTC would be expected. These two factors may explain why activation energy of OTC sorption to magnetite was slightly higher at 0.5 M I than that of 0.01 M I. In our earlier work, it was documented that at low surface coverage (i.e., below 1 mM initial OTC concentration), I effect was negligible and the sorption occurred via inner-sphere mechanism, whereas at high surface coverage (i.e., at 2 mM initial OTC concentration), I effect was somewhat noticeable (Rakshit et al. 2013). The faster kinetics at higher temperature in the case of higher I was consistent with the above finding (Fig. 3).

Activation energy value (E_{a}) below 42 kJ mol^{-1} generally suggests a diffusion-controlled process, and a higher value indicates a surface chemical-controlled reaction (Sparks 1989). The determined E_{a} s in our study at both I s are either higher or close to this value (Table 2), suggesting negligible contribution of diffusion in sorption kinetics. The enthalpy of activation ($\Delta H^{\ddagger}$) for both I s indicated that the sorption process is endothermic, and consumed energy (Table 2). The entropy of activation ($\Delta S^{\ddagger}$) calculated from the Eyring equation (Eq. 6; Fig. 4a, b) suggested that the sorption process occurred via an associative mechanism. Associative reaction mechanism suggests that an intermediate of higher coordination number is formed between the entering group (i.e., OTC) and magnetite. Generally, a value of $\Delta S^{\ddagger} < -10$ J mol^{-1} K^{-1} is indicative of associative reaction mechanism and a value $> +10$ J mol^{-1} K^{-1} suggests a dissociative reaction mechanism (Atwood 1985). The enthalpy of sorption (ΔH_{ad}) calculated from the van't Hoff equation (Eq. 9) resulted in a large and positive value for both I s. A large positive value of ΔH_{ad} is indicative of inner-sphere surface complexation (Journey et al. 2010). An exact magnitude of ΔH_{ad} to separate inner- and outer-sphere sorption has not yet been established (Journey et al. 2010). Likewise, if $T\Delta S_{\mathrm{ad}}$ is a large

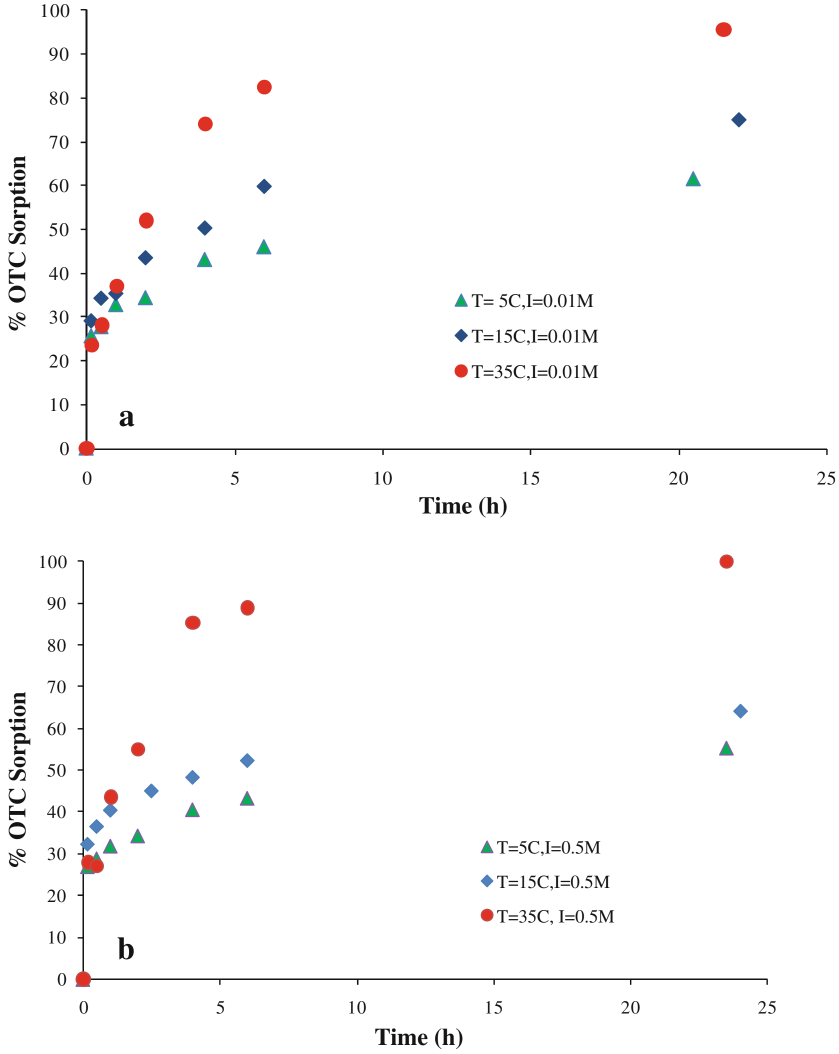

Fig. 2 **a** Sorption kinetics of OTC on 20 g L^{-1} magnetite at three different temperatures at an ionic strength of 0.01 M and a buffered pH of 5.55. **b** Sorption kinetics of OTC on 20 g L^{-1} magnetite at three different temperatures at an ionic strength of 0.5 M and a buffered pH of 5.55

Table 1 Pseudo-first-order rate coefficients for OTC sorption on magnetite at different ionic strengths and pH values

Experimental conditions (M)	Pseudo-first-order rate coefficients		
	5C[a] (s^{-1})	15C[a] (s^{-1})	35C[a] (s^{-1})
$I = 0.01$	2×10^{-5} ($R^2 = 0.96$)	3×10^{-5} ($R^2 = 0.98$)	8×10^{-5} ($R^2 = 0.99$)
$I = 0.5$	1×10^{-5} ($R^2 = 0.97$)	2×10^{-5} ($R^2 = 0.94$)	1×10^{-4} ($R^2 = 0.96$)

[a] Temperature in Celsius

Table 2 Thermodynamic parameters for OTC sorption on magnetite at two ionic strength values

Experimental conditions (M)	E_a (kJ mol^{-1})	$\Delta H^{\ddagger}$ (kJ mol^{-1})	$\Delta G^{\ddagger}$ at 25 °C (kJ mol^{-1}	$\Delta S^{\ddagger}$ (J mol^{-1} K^{-1})	ΔH_{ad} (kJ mol^{-1})	ΔS_{ad} (J mol^{-1} K^{-1})	ΔG_{ad} at 25 °C (kJ mol^{-1})
$I = 0.01$	33.29	30.84	114.48	−280.68	170.09	590	−5.06
$I = 0.5$	55.20	52.76	114.78	−208.11	228.19	800	−8.79

contributor to ΔG_{ad} compared to ΔH_{ad}, the sorption reaction is thought to be driven by entropy and via chemisorption (Journey et al. 2010). The ΔS_{ad} value in Table 2 suggested that the OTC sorption by magnetite was entropically driven. This indicates that the sorption process likely occurred via inner-sphere mechanism at both I s.

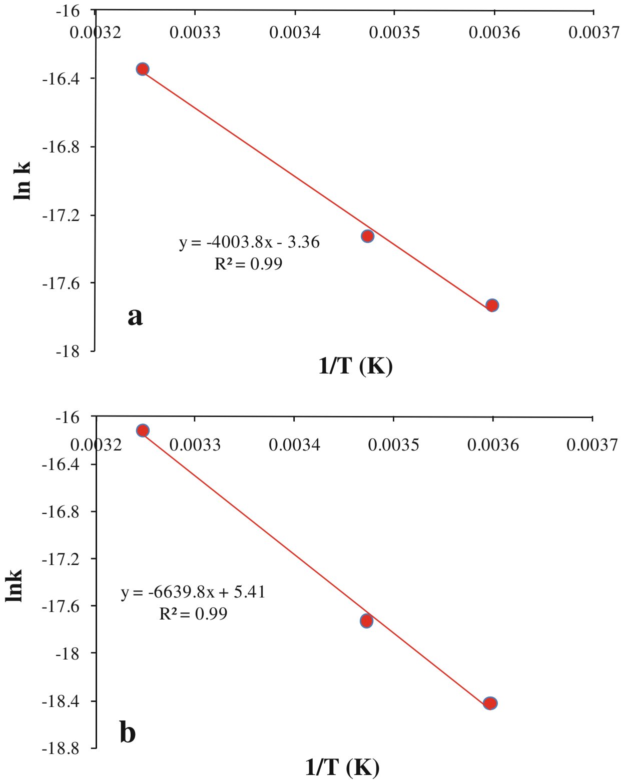

Fig. 3 **a** Arrhenius *plot* of the temperature dependence of OTC sorption by magnetite at an ionic strength of 0.01 M. **b** Arrhenius *plot* of the temperature dependence of OTC sorption by magnetite at an ionic strength of 0.5 M

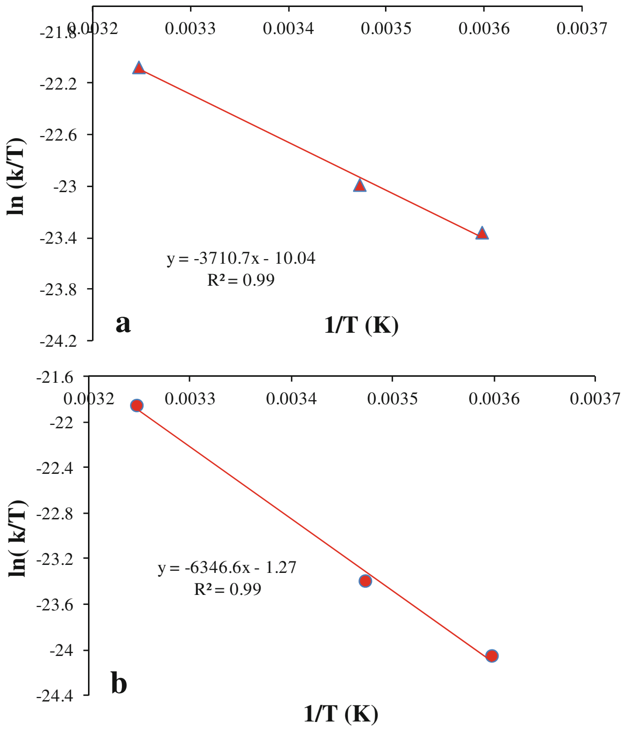

Fig. 4 **a** Eyrings *plot* of the temperature dependence of OTC sorption by magnetite at an ionic strength of 0.01 M. **b** Eyrings *plot* of the temperature dependence of OTC sorption by magnetite at an ionic strength of 0.5 M

Therefore, although some *I* effect was noticed in the sorption kinetics, the overall sorption did not suggest any clear contribution from outer-sphere process. The overall ΔG_{ad} of the sorption reaction did not show a marked difference between the two *I* s (Table 2). However, overly mechanistic interpretations from thermodynamic data cannot be justified due to its inherent nature of origin from empirical kinetic equations.

Reaction order and rate constant

The reaction order with respect to [OTC] was 1.24 and with respect to magnetite surface site concentration was 0.75 (Fig. 5a, b). The total surface site concentration of 20 g L^{-1} magnetite was 6.9×10^{-3} mol L^{-1} (Rakshit et al. 2013). The initial concentration of OTC varied between 0.25 and 1 mM and that of magnetite varied between 2.5 and 20 g L^{-1} while pH was kept constant at 5.55. Rubert and Pedersen (2006) reported reaction orders for OTC and MnO_2 as 0.8 and 0.7, respectively, at a pH value of 5.6 in their study of OTC transformation by MnO_2. For the determination of reaction order for [H^+], pH was varied from 3.8 to 7.6 while maintaining OTC initial concentration at 1 mM and magnetite surface site concentration at 6.9×10^{-3} mol L^{-1} (i.e., 20 g L^{-1} magnetite). As mentioned earlier, data were fitted using the reaction staring from 10 min. Therefore, the initial fast sorption step was not included in data analysis. A similar method of data analysis was conducted by Wehrli et al. (1990) who also observed a very fast initial sorption step for vanadyl sorption to aluminum oxide.

The reaction order for [H^+] could not be determined because of a nonlinear dependence of the pseudo-first-order rate constant (Fig. 6). This could be due to the fact that the pH dependence of the sorption rate is very complex. In fact, in our earlier work, we found that four surface complexation reactions were required to model the pH dependence of the sorption process (Rakshit et al. 2013) as follows:

$$\mathrm{XOH} + \mathrm{OTC}^{2-} = \mathrm{XOTC}^{-} + \mathrm{OH}^{-} \; \log K^{\mathrm{int}} = 15.30 \tag{10}$$

$$2\mathrm{XOH} + \mathrm{OTC}^{2-} = \mathrm{X_2OTC} + 2\mathrm{OH}^{-} \; \log K^{\mathrm{int}} = 23.19 \tag{11}$$

$$2\mathrm{XOH} + 2\mathrm{OTC}^{2-} = \mathrm{X_2(OTC)_2^{2-}} + 2\mathrm{OH}^{-} \; \log K^{\mathrm{int}} = 22.89 \tag{12}$$

$$\mathrm{XOH} + 2\mathrm{OTC}^{2-} = \mathrm{X(OTC)_2^{3-}} + \mathrm{OH}^{-} \; \log K^{\mathrm{int}} = 32.77 \tag{13}$$

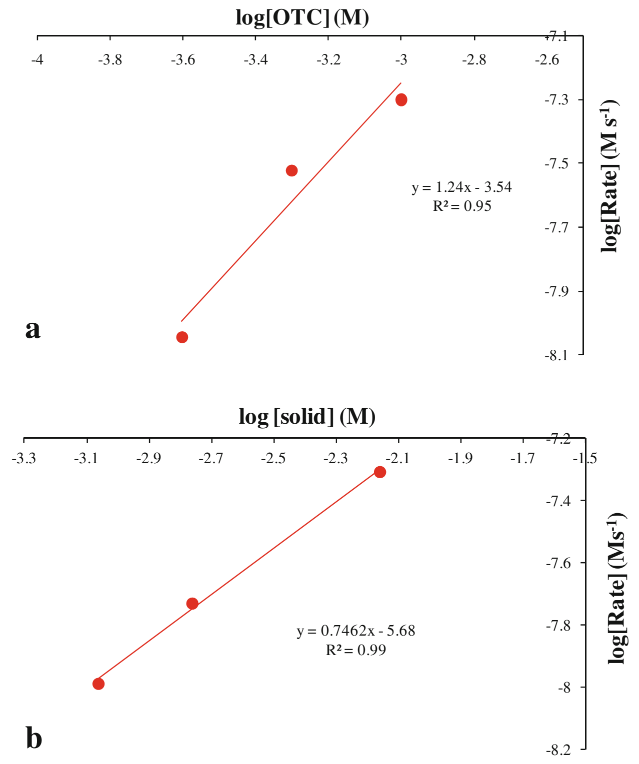

Fig. 5 **a** Initial rate *plots* to determine apparent reaction order at OTC concentrations of 0.25, 0.5, and 1 mM. The pH value was fixed at 5.45, and Fe_3O_4(s) concentration was 20 g L^{-1}. The *solid line* represents a linear least square regression fit of the data. **b** Initial rate *plots* to determine apparent reaction order at nano-Fe_3O_4 concentrations of 2.5, 5, and 20 g L^{-1}. The pH value was fixed at 5.45. The *solid line* represents a linear least square regression fit of the data

where XOH is the magnetite surface, and OTC is oxytetracycline. The K^{int} values represent the fitted intrinsic equilibrium constants for a given reaction.

It is implied by these reactions that a dinegative OTC species was involved in OTC sorption. Because OTC speciation at low pH is dominated by its positive and neutral species, the OTC solution speciation equilibrium has to shift toward producing more OTC^{2-} species (Rakshit et al. 2013). Therefore, it follows that as long as a positive surface exists, the sorption reaction rate would be slower at lower pH and faster at higher pH. This is noticed in the k_{obs} versus pH plot at pH 3.8, 5.9, and 6.45 (Fig. 6). The decrease in k_{obs} at pH 7.6 can be explained by the fact that the magnetite surface became increasingly negative at that pH. It should be noted that the kinetic behavior of sorption ought not to be confused with amount of OTC sorbed at equilibrium. Higher OTC sorption at lower pH compared to that at higher pH was noticed in our earlier work. Therefore, it is possible that once the initial kinetic barrier is overcome, the system is stabilized more at lower pH.

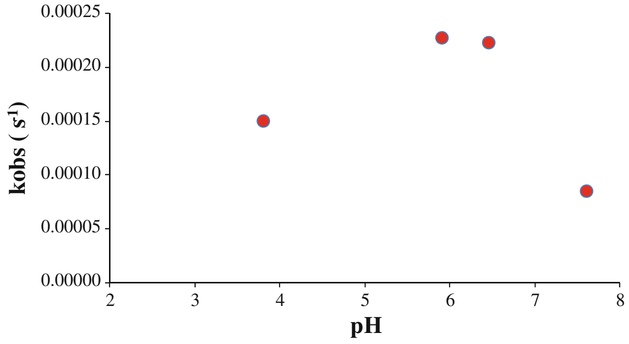

Fig. 6 The relationship of pseudo-first-order rate coefficients with pH

Using the empirical reaction order coefficients of OTC and magnetite, the overall rate equation can be written as:

$$-d[\mathrm{OTC}]/\mathrm{d}t = k_3[\mathrm{OTC}]^{1.24}[\mathrm{XOH}]^{0.76} \qquad (14)$$

where k_3 = initial reaction rate constant at pH 5.55.

Since k_3 depends on pH, the rate constant at a given pH can be determined by following equation:

$$k_{3,\,\mathrm{pH}5.55} = \{-d[\mathrm{OTC}]/\mathrm{d}t\}/\left\{[\mathrm{OTC}]^{1.24}[\mathrm{XOH}]^{0.76}\right\} \qquad (15)$$

At pH 5.55, the rate $\{-d[\mathrm{OTC}]/dt\}$ is $= 5 \times 10^{-8}$ M s^{-1}, initial OTC concentration = 0.001 M, and magnetite surface site concentration = 6.9×10^{-3} mol L^{-1}. From Eq. (15), the value of k_3 can be determined in the above conditions. Therefore, $k_{3,\mathrm{pH}5.55} = (5 \times 10^{-8})/\{(0.001)^{1.24} \quad (6.9 \times 10^{-3})^{0.76}\} = 1.15 \times 10^{-2}$ M^{-1} s^{-1}. Similarly, the value of k_3 at other pH values can be determined.

Conclusion

This study provides important information on the kinetics of OTC sorption on nano-Fe_3O_4. The data on the temperature dependence of the reaction rate coefficient will be useful in understanding the environmental mobility of OTC in summer and winter seasons where magnetite is a dominant iron oxide mineral. For example, in magnetite-rich soils, the rate of OTC removal will be ten times faster at 35 °C than at 5 °C. Treatment technologies designed to use nano-magnetite as a remediation material for OTC will perform better at higher temperature. Because the effect of *I* on the reaction rate was found to be negligible at the temperature range of 5–35 °C, fertilizer application will most likely not affect OTC sorption kinetics on magnetite. However, the effect of common anions such as $H_2PO_4^-$, NO_2^-, and NO_3^- on OTC sorption by magnetite needs to be studied in order to understand the effect of fertilizers accurately. Although we could not derive a pH-independent rate constant for OTC sorption kinetics for nonlinear dependence of reaction rate with pH, the OTC removal rate at a specific pH can be determined using Eq. (15). This will provide important information to soil scientists trying to predict the fate of the VA, OTC in an iron oxide-rich soil, as well as to the environmental engineers designing a wastewater treatment system for the human antibiotic, OTC, using nano-magnetite as the remediation material.

Acknowledgments The authors thank Dr. Laying Wu of Montclair State University for her help with TEM analysis.

References

Atwood JD (1985) Inorganic and organometallic reaction mechanisms. VCH, New York

Boxall ABA, Blackwell P, Cavallo R, Kay P, Tolls J (2002) The sorption and transport of a sulphonamide antibiotic in soil systems. Toxicol Lett 131:19–28

Boxall A, Kolpin DW, Halling-Sørensen B, Tolls J (2003) Are veterinary medicines causing environmental risks? Environ Sci Technol 37:286A–294A

Chang P-H, Li Z, Yu T-L, Munkhbayer S, Kuo T-H, Hung Y-C, Jean JS, Lin K-H (2009) Sorptive removal of tetracycline from water by palygorskite. J Hazard Mater 165:148–155

Chu B, Goyne KW, Anderson SH, Lin C-H, Udawatta RP (2010) Veterinary antibiotic sorption to agroforestry buffer, grass buffer and cropland soils. Agrofor Syst 79:67–80

Crane RA, Dickison M, Popescu IC, Scott TB (2011) Magnetite and zero-valent iron nanoparticles for the remediation of uranium contaminated environmental water. Water Res 45:2931–2942

Davis JG, Truman CC, Kim SC, Ascough JC II, Carlson K (2006) Antibiotic transport via runoff and soil loss. J Environ Qual 35:2250–2260

Figueroa RA, Mackay AA (2005) Sorption of oxytetracycline to iron oxides and iron oxide-rich soils. Environ Sci Technol 39:6664–6671

Fritz JW, Zuo Y (2007) Simultaneous determination of tetracycline, oxytetracycline, and 4-epitetracycline in milk by high-performance liquid chromatography. Food Chem 105:1297–1301

Furukawa Y, Kim J-W, Watkins J, Wilkin RT (2002) Formation of ferrihydrite and associated iron corrosion products in permeable reactive barriers of zero-valent iron. Environ Sci Technol 36:5469–5475

Gu C, Karthikeyan KG (2005) Interaction of tetracycline with aluminum and iron hydrous oxides. Environ Sci Technol 39:2660–2667

Hamscher G, Sczesny S, Hoper H, Nau H (2002) Determination of persistent tetracycline residues in soil fertilized with liquid manure by high-performance liquid chromatography with electrospray ionization tandem mass spectrometry. Anal Chem 74:1509–1518

Hays KF, Papelis C, Leckie J (1988) Modeling ionic strength effects on anion adsorption at hydrous oxide/solution interfaces. J Colloid Interface Sci 125:717–726

Jones AD, Bruland GL, Agrawal SG, Vasudevan D (2005) Factors influencing the sorption of oxytetracycline to soils. Environ Toxicol Chem 24:761–770

Journey JS, Anderson RM, Essington ME (2010) The adsorption of 2-ketogluconate by goethite. Soil Sci Soc Am J 74:1119–1128

Keleti T (1983) Errors in the evaluation of Arrhenius and van't Hoff plots. Biochem J 209:277–280

Kolpin DW, Furlong ET, Meyer MT, Thurman EM, Zaugg SD, Barber LB, Buxton HT (2002) Pharmaceuticals, hormones, and other organic wastewater contaminants in US stream, 1999–2000: a national reconnaissance. Environ Sci Technol 36:1202–1211

Kulshrestha P, Giese RF, Aga DS (2004) Investigating the molecular interactions of oxytetracycline in clay and organic matter: insights on factors affecting its mobility in soil. Environ Sci Technol 38:4097–4105

Kummerer K (2009) Antibiotics in the aquatic environment—a review—part I. Chemosphere 75:417–434

Lasaga AC (1981) Rate laws of chemical reactions. In: Lasaga AC, Kirkpatrick RJ (eds) Kinetics of geochemical processes, reviews in mineralogy, vol 8. Mineralogical Society of America, Washington, DC, pp 1–68

Nagayama M, Cohen M (1962) The anodic oxidation of iron in neutral solution: 1. The nature and composition of the passive film. J Electrochem Soc 109:781–790

Phillips DH, Gu B, Watson DB, Roh Y (2003) Impact of sample preparation on mineralogical analysis of zero-valent iron reactive barrier materials. J Environ Qual 32:1299–1305

Pils JRV, Laird DA (2007) Sorption of tetracycline and chlortetracycline on K- and Ca-saturated soil clays, humic substances, and clay-humic complexes. Environ Sci Technol 41:1928–1933

Rabolle M, Spliid NH (2000) Sorption and mobility of metronidazole, olaquindox, oxytetracycline and tylosin in soil. Chemosphere 40:715–722

Rakshit S, Sarkar D, Elzinga E, Punamiya P, Datta R (2013) Sorption of oxytetracycline on magnetite-water interface. Appl Geochem (in revision)

Rubert KI, Pedersen JA (2006) Kinetics of oxytetracycline reaction with a hydrous manganese oxide. Environ Sci Technol 40:7216–7221

Scheckel KG, Sparks DL (2001) Temperature effects on nickel sorption kinetics at the mineral-water interface. Soil Sci Soc Am J 65:719–728

Schwarzenbach RP, Escher BI, Fenner K, Hofstetter TB, Johnson CA, von Gunten U, Wehrli B (2006) The challenge of micropollutants in aquatic systems. Science 313:1072–1077

Scott TB, Dickison M, Crane RA, Riba OR, Hughes G (2010) The effects of vacuum annealing on the structure and surface chemistry of iron nanoparticles. J Nanopart Res 12:1765–1775

Sparks DL (1989) Kinetics of soil chemical processes. Academic Press, San Diego

Stumm W, Morgan JJ (1996) Aquatic chemistry, 3rd edn. Wiley, New York

Tolls J (2001) Sorption of veterinary pharmaceuticals in soils: a review. Environ Sci Technol 35:3397–3406

Vasudevan D, Bruland GL, Torrance BS, Upchurch VG, MacKay AA (2009) pH-dependent ciprofloxacin sorption to soils: interaction mechanisms and soil factors influencing sorption. Geoderma 151:68–76

Wang Y, Morin G, Ona-Naguema G, Juillot F, Calas G, Brown GE Jr (2011) Distinctive arsenic (V) trapping modes by magnetite nanoparticles induced by different sorption process. Environ Sci Technol 45:7258–7266

Watkinson AJ, Murby EJ, Costanzo SD (2007) Removal of antibiotics in conventional and advanced wastewater treatment: implications for environmental discharge and wastewater recycling. Water Res 41:4164–4176

Wehrli B, Ibric S, Stumm W (1990) Adsorption kinetics of vanadyl (IV) and chromium (III) to aluminum oxide: evidence for a two step mechanism. Colloid Surf 51:77–88

Yang W, Kan AT, Chen W, Tomson MB (2010) pH-dependent effect of zinc on arsenic adsorption to magnetite nanoparticles. Water Res 44:5693–5701

Zhang D, Niu H, Zhang X, Meng Z, Cai Y (2011) Strong adsorption of chlorotetracycline on magnetite nanoparticles. J Hazard Mater 192:1088–1093